Stimulation of various forms of stress corrosion in an austenitic stainless steel

ANTONIO ALDERISIO, BRUNO BREVAGLIERI, STEFANO NATALI, GIUSEPPE SIGNORELLI - Dipartimento di Ingegneria Chimica, dei Materiali, delle Materie Prime e Metallurgia, Sede di Metallurgia, Facoltà di Ingegneria, Università La Sapienza, Rome, Italy

Abstract

A heat-treated AISI 304 austenitic stainless steel has been studied in a 1N H_2SO_4 + 0.2N NaCl solution at constant load and at room temperature and 80°C.

The SEM examination has been used to ascertain the morphology and evolution of attack, initiated at preformed pits having critical dimensions, owing to the effect of polarization in the imperfect passivity zone and subsequently, alternatively in the regions of perfect passivity, active-passive transition, activity and in freely-corroding conditions. Reverse and direct polarization sequences have been investigated.

It has been observed that in some cases the integranular mode of attack changes to transgranular. In other cases it is intensified. While in yet others it is depressed. Attack that is initially transgranular cannot be modified to intergranular.

With the methodologies applied it has been possible at will to induce the appearance of various stress-corrosion cracking forms or to ensure the degeneration thereof into other forms of attack.

Riassunto

È stato studiato un acciaio inossidabile austenitico AISI 304 nello stato solubilizzato, in una soluzione di prova costituita da H_2SO_4 1N + NaCl 0,2N, sotto un carico costante, a temperatura ambiente e a 80°C.

Mediante osservazioni al microscopio a scansione è stata studiata la morfologia e l'evoluzione dell'attacco, innescato in corrispondenza di cavità performate con dimensioni critiche, per effetto della polarizzazione nella zona di passività imperfetta e successivamente, in alternativa tra loro, nelle regioni di passività perfetta, di transizione attivo-passiva, di attività e di libera corrosione. Sono state sperimentate sequenze di polarizzazione inverse, oltre che dirette.

È stato osservato che in alcuni casi l'andamento intergranulare dell'attacco si modifica in transgranulare, in altri casi esso è esaltato, in altri ancora è depresso; un attacco inizialmente transgranulare non è modificabile in uno intergranulare.

Con la metodologia sperimentata è possibile provocare ad arte la comparsa di forme diverse di tensocorrosione, oppure la sua degenerazione in altre forme di attacco.

Introduction

Stress corrosion occurs when the dissolution rate of the slip steps and that of their formation are comparable.

The rate of formation of the slip steps depends on the dynamic strain rate, and on the stress applied in the constant load tests. The corrosion rate of the slip steps depends on the corrosiveness of the environment. When the former prevails over the latter, the formation of steps is observed; their dissolution constitutes the control stage of the overall process [1-3].

In kinetically easy passivation conditions, under the applied loads the dislocations slip and pile-up on the grain boundaries, acting as stress raisers and hence favouring intergranular dissolution.

By keeping the load and also the slip-step formation rate constant, dissolution rates that are higher or lower than that of their formation can be obtained by modifying the passivation behaviour of the steel through appropriate variations in potential and/or temperature.

As previously observed [4] and as borne out by other workers [5], by taking action on these parameters various forms of stress corrosion are established, or degeneration of the phenomenon is induced with the generation of other forms such as pitting corrosion, sometimes with very deep pits or tunnels [6], or even general attack.

The research reported here was performed to check on these points. The work involved examination under the scanning electron microscope to study the morphology and evolution of corrosion on samples containing intergranular microcracks produced by polarization in the imperfect passivity region, and subsequently polarized in the regions of perfect passivity, active-passive transition and activity, as well as the freely-corroding condition.

Materials and equipment

The study was concentrated on an AISI 304 austenitic stainless steel whose composition (%wt) was C 0.041, Cr 18.60, Ni 8.80, Mn 1.05, Si 0.30, P 0.004, S 0.005 and Mo 0.35.

The tensile test specimens were 15 mm long and 4 mm in diameter. After working they were heat treated at 1050°C for thirty minutes and water quenched. The oxide and the chromium depleted layer were then removed by rough grinding and the desired surface finish was acquired by treatment with wet 1000-grade CSi paper.

The test solution consisted of 1N $H_2SO_4+0.2N$ NaCl [7]. The tests were run at room temperature and 80°C.The samples were stressed by a constant tensile load equal to 80% $\sigma_{p(O.2)}$.

The electrochemical tests were carried out using an AMEL Corrograph, with a saturated calomel electrode (SCE).

The samples were examined under a Hitachi S 2500 scanning electron microscope (SEM).

Methodology and experimental results

The experiments were conducted within the potential ranges described by the cyclic polarization curve illustrated in Fig. 1. New pits are formed and those already formed are enlarged at potentials more noble than E_R, breakdown potential, (Stage 1).

This phase is common to all the tests in the research reported here. In actual fact, it has been ascertained [4, 8-11] that stress corrosion cracking often starts when pitting corrosion and crevice corrosion are active, because pits and crevices act as stress raisers, favouring crack nucleation.

In the $E_R \div E_P$ (protection potential) range — imperfect passivity region (Stage 2) where pre-existing pits grow — polarization was effected at +850 mV in the room temperature tests and at +20 mV in those at 80°C.

Perfect passivity occurs between E_P and E_p, passive potential (Stage 3).

Between E_p and E_{pp} (primary passive potential) there is an active-passive zone (Stage 4). At room temperature and 80°C, polarization was performed at −100 mV.

Between E_{pp} and E_{corr} (corrosion potential) there is an active zone (Stage 5). The potentials selected for polarization here were −350 mV in the room temperature tests and −320 mV in those at 80°C.

Stage 6 represents the freely corroding condition. During the test the corrosion potential, measured after 5 minutes immersion, shifts until the value becomes stationary.

The experiments were conducted by adopting the combinations described in Table I, under various experimental conditions.

Stage 1, common to all the experiments, consisted in anodic polarization at potentials more noble than E_R with passage of a 10 mA current (exposed surface = 4 cm^2) for 30 min, at room temperature, so as to obtain numerous pits with critical dimensions, effective for microcrack initiation [4].

In the experiments involving combination (125) the specimen exhibits intergranular and transgranular attack on the bottom of the preformed pits, as illustrated in Fig. 2.

More prolonged polarization in the active field causes the disappearance of intergranular attack and the accentuation of the transgranular mode of cracking (Fig. 3).

In the reverse combinations (152) corrosion is devastating, with the formation of caverns [6, 7, 12], as illustrated in Fig. 4.

In the (124) sequences, intergranular attack on the bottom of the crack, typical of Stage 2, disappears almost completely, as amply demonstrated in earlier research [4, 7]. Fig. 5a documents the morphology

Table 1 - Experimental conditions

Combinat.	Stage	Temp.	Duration	Poten.	Stage	Temp.	Duration	Poten.
		°C	h	mV		°C	h	mV
(125 A)	2	20	42	+850	5	80	7	−350
(125 B)	2	20	117	+850	5	80	3	−350
(125 C)	2	20	93	+850	5	80	6	−350
(125 D)	2	20	62	+850	5	80	5	−350
(125 E)	2	20	121	+850	5	80	6	−350
(125 F)	2	20	66	+850	5	20	8	−350
(125 G)	2	20	80	+850	5	20	10	−350
(125 H)	2	80	10	+20	5	20	10	−350
(125 I)	2	80	10	+10	5	80	3	−320
(152 A)	5	80	21	−320	2	20	120	+850
(152 B)	5	20	20	−350	2	20	60	+850
(124 A)	2	20	140	+850	4	20	4	+100
(124 B)	2	20	120	+850	4	20	7	−100
(124 C)	2	20	120	+850	4	20	10	−100
(142 A)	4	20	20	−100	2	20	120	+850
(142 B)	4	20	30	−100	2	20	120	+850
(14)	4	20	20	−100				
(13)	3	20	30	+200				
(126 A)	2	20	160	+850	6	20	45	—
(126 B)	2	20	120	+850	6	20	50	—
(126 C)	2	20	120	+850	6	20	30	—
(162 A)	6	20	140	—	2	20	170	+850
(162 B)	6	20	100	—	2	20	120	+850
(16 A)	6	20	100	—				
(16 B)	6	80	15	—				

of this intergranular attack, while 5b illustrates the survival of a residue of intergranular attack on the bottom of the pit.

The result of the reverse combinations (142) is intensification of the intergranular attack typical of

Stage 2, as documented by Fig. 6.

The attack morphology documented by Fig. 7 is representative of the (126) sequences. Here the general attack, characteristic of Stage 6, is superimposed on intergranular attack. In the reverse sequences (162) only intergranular attack appears.

Combinations (13), (14) and (16) produced no attack that can be classed as stress corrosion cracking, the latter case also being confirmed by Bilogan [13].

Test temperature was chosen bearing in mind the fact that it influences the process rate and not attack morphology.

Discussion

Inter- and transgranular attack have been observed in all the experiments characterized by the (125) sequence. However, these are not produced simultaneously; indeed, the latter occurs after the former. The transgranular mode of cracking — an effect characteristic of polarization in the active zone (Stage 5) — initiates on the boundary of grains attacked in the previous Stage 2 (polarization in the imperfect passivity region), when experimental conditions move to the active field.

In previous research [4, 7] the simultaneous presence of these two forms of attack was noted as the result of the polarization at potentials in the imperfect passivity region, but in a substantially different way. Namely, together with an intergranular mode of cracking, there were signs characteristic of transgranular attack, i.e. parallel grooves and fine parallel pleats.

Fig. 2 illustrates the morphology of the attack observed in combination (125 B), where polarization in the active field was brief (3 h). Longer exposure (6 h) caused the almost total disappearance of intergranular attack and accentuation of the transgranular mode of cracking (Fig. 3a and b) with the combination (125 C).

The corrosion resulting from the reverse combination (152) is quite different. A transgranular mode of cracking cannot be changed into an intergranular mode. On passing from active to passive conditions the crack degenerates into diverse corrosion forms, with the appearance of pits and tunnels (Fig. 4).

With the (124) sequence, prolonged exposure to the corrosive environment, in a potential range where anodic current intensity is fairly high, results in the almost complete elimination of signs of intergranular attack (Fig. 5).

Diversely, with the (142) combination, final intergranular attack, documented by Fig. 6, is much more marked than that of the (12) sequence; it seems as if Stage 4 causes marked sensitization to intergranular attack.

As a result of combination (126) it is observed that superimposed on the typical intergranular attack of Stage 2 there is a weak form of general attack, precisely of the freely corroding condition, which is insufficient to mask the previous attack.

Only general attack occurs with the reverse sequence (162).

With combinations (13) and (14) there is no stress corrosion in the conditions employed.

Comparison of the corrosion that occurs with the three reverse sequences (152), (142) and (162) indicates that intergranular stress corrosion cracking is initiated only with the second combination. Initial active conditions (Stage 5) or freely corroding conditions (Stage 6) seem to prevent the occurrence of this phenomenon. In actual fact, only the (142) combination brings about the active-passive condition in Stage 4, thus predisposing the steel to intergranular stress corrosion cracking which starts and proceeds markedly in the successive Stage 2.

Active or freely corroding conditions instead, lead to attack rates that are too high to be compatible with the onset of intergranular stress corrosion cracking owing to the effect of polarization in the imperfect passive region.

In the direct sequences (125), (124) and (126), intergranular attack, produced in Stage 2, is partially or totally blocked, depending on the type and duration of the ensuing polarization.

Stage 5 tends to cancel the results of intergranular attack, initiating the transgranular mode of cracking, typical of this potential range under the conditions employed.

The other two stages, 4 and 6, cause milder selective attack conditions, and tend respectively to cancel the integranular attack figures and to superimpose on them.

The (125) sequence effectively simulates the succession of processes, reproducing the effects that occur in localized corrosion of austenitic steels in chloride environment on passing from the free-surface passive potentials to the in-pit active potentials as per the model proposed by Seys et al. [14]. Stress corrosion cracking, therefore, is represented as a specific case of pitting corrosion.

Conclusions

Various kinds of stress corrosion forms can be produced in an austenitic stainless steel, depending on the conditions to which it is subjected.

In the research reported here, this result has been obtained by acting on anodic polarization, namely by polarizing in diverse regions and performing a variety of polarization sequences. In this manner, action has been taken on the passivation of the steel, thus varying the rate of attack of the slip-steps formed as a result of the loads applied, and hence obtaining a variety of attack morphologies all typical of stress corrosion cracking.

In particular, sequence (125) — consisting in the formation of mini-pits, polarization in the imperfect passivity zone and then in the active region — effectively simulates the succession of stages followed by stress corrosion cracking initiated at a pit, namely, (a) pit formation, (b) intergranular attack on the bottom of the pit, (c) evolution of the crack from inter- to transgranular.

This methodology appears useful for identifying and reproducing the real phenomena under diverse experimental conditions, with satisfactory reproducibility, in a relatively brief space of time and with the use of a limited number of samples.

References

[1] M. Takano, Corrosion, 30, (12), 441-446, 1974;
[2] H. Okada, Y. Hosoi, S. Abe, Corrosion, 27, (10), 424-428, 1971;
[3] T. Nakayama, M. Takano, Corrosion, 38, (1), 1-9, 1982;
[4] A. Alderisio, B. Brevaglieri, G. Signorelli, Metall. Sci. Technol., 7, (1), 76-83, 1989;
[5] G.S. Duffó, I.A. Maier, J.R. Galvele, Corros. Sci., 28, (10), 1003-1018, 1988;
[6] J.D. Harston, J.C. Scully, Corrosion, 25, (12), 493-501, 1969;
[7] A. Alderisio, M. Bianchi, B. Brevaglieri, G. Signorelli, Metall. Sci. Technol., 6, (1), 3-6, 1988;
[8] R.N. Parkins, Met. Technol., 9, 122-129, 1982;
[9] Z. Szklarska-Smialowska, Films and Their Importance in the Nucleation of Stress Corrosion Cracking in Stainless Steel, from Hydrogen Embrittlement and Stress Corrosion Cracking, ed. R. Gibala, R.F. Hehemann, 207-229, ASM, 1984;
[10] Z. Szklarska-Smialowska, J. Gust, Corros. Sci., 19, 753-765, 1979;
[11] G. Cragnolino, L.F. Lin, Z. Szklarska-Smialowska, Corrosion, 37, (6), 312-320, 1981;
[12] A. Honkasalo, Corrosion, 29, (6), 237-240, 1973;
[13] K. Bilogan, Corrosion, 39, (8), 323-329; 1983;
[14] A.A. Seys, M.J. Brabers, A.A. Van Haute, Corrosion, 30, (2), 47-52, 1974.

Figure captions

Fig. 1: Cyclic polarization curve in 1N $H_2SO_4 + 0.2N$ NaCl, under load at room temperature. Legend. Zones of anodic polarization: (1) Pitting, (2) Imperfect Passivity, (3) Perfect Passivity, (4) Active-Passive Transition, (5) Active; (6) Cathodic Polarization.

Fig. 2: Inter- and transgranular attack on bottom of preformed pit. Sequence (125 B), $\times 1000$.

Fig. 3: Transgranular mode of cracking, sequence (125 C): (a) $\times 200$, (b) $\times 3500$.

Fig. 4: Pit with metallic residues in the form of platelets. Sequence (152 A), $\times 40$.

Fig. 5: Superimposition of general attack on intergranular attack (124 A): (a) Attenuation of original attack, $\times 3000$, (b) disappearance thereof $\times 1500$.

Fig. 6: Intensification of intergranular attack. Sequence (142), $\times 1000$.

Fig. 7: Superimposition of general attack under freely corroding conditions on intergranular attack. Sequence (126 A), $\times 1000$.

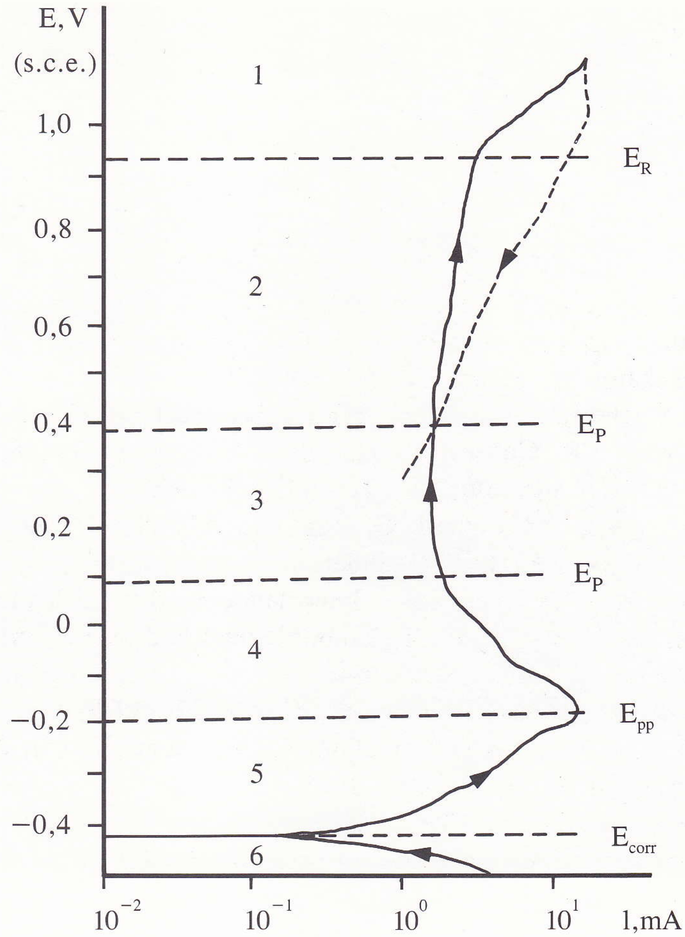
E,V
(s.c.e.)
1,0
0,8
0,6
0,4
0,2
0
−0,2
−0,4
1
2
3
4
5
6
E_R
E_P
E_P
E_{pp}
E_{corr}
10^{-2}
10^{-1}
10^{0}
10^{1}
1,mA

Fig. 1

Fig. 2

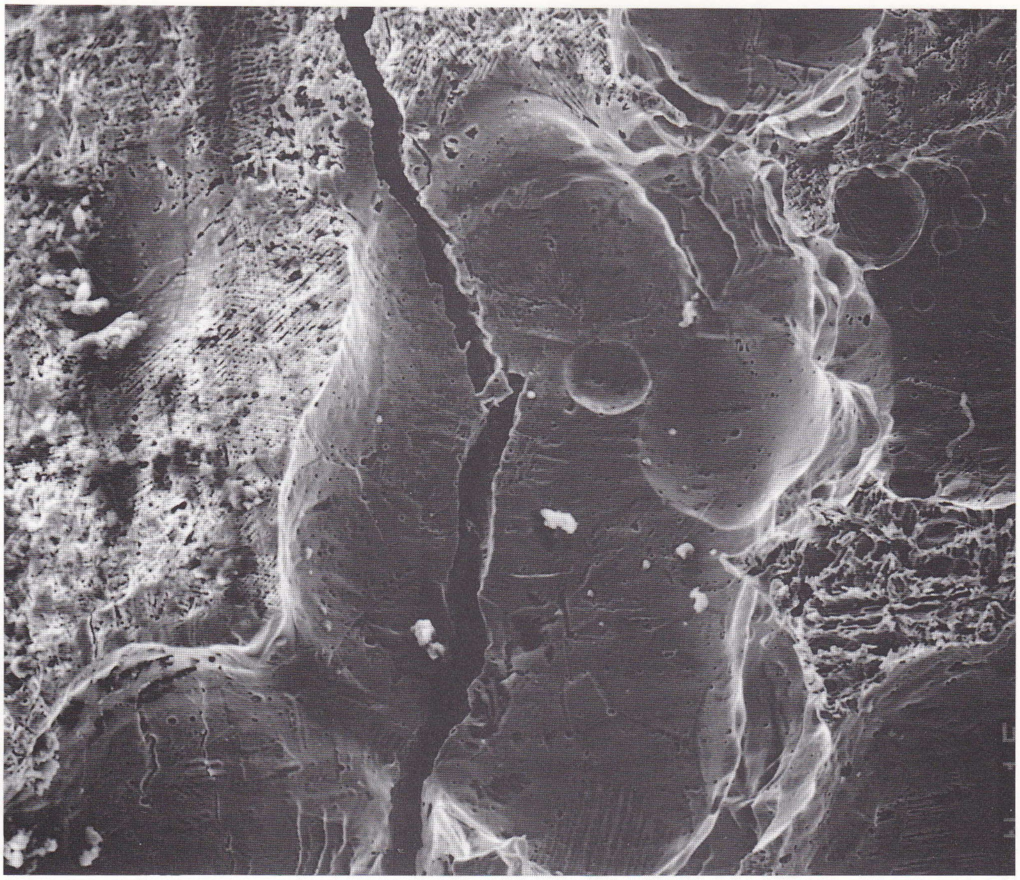

Fig. 3a

Fig. 3b

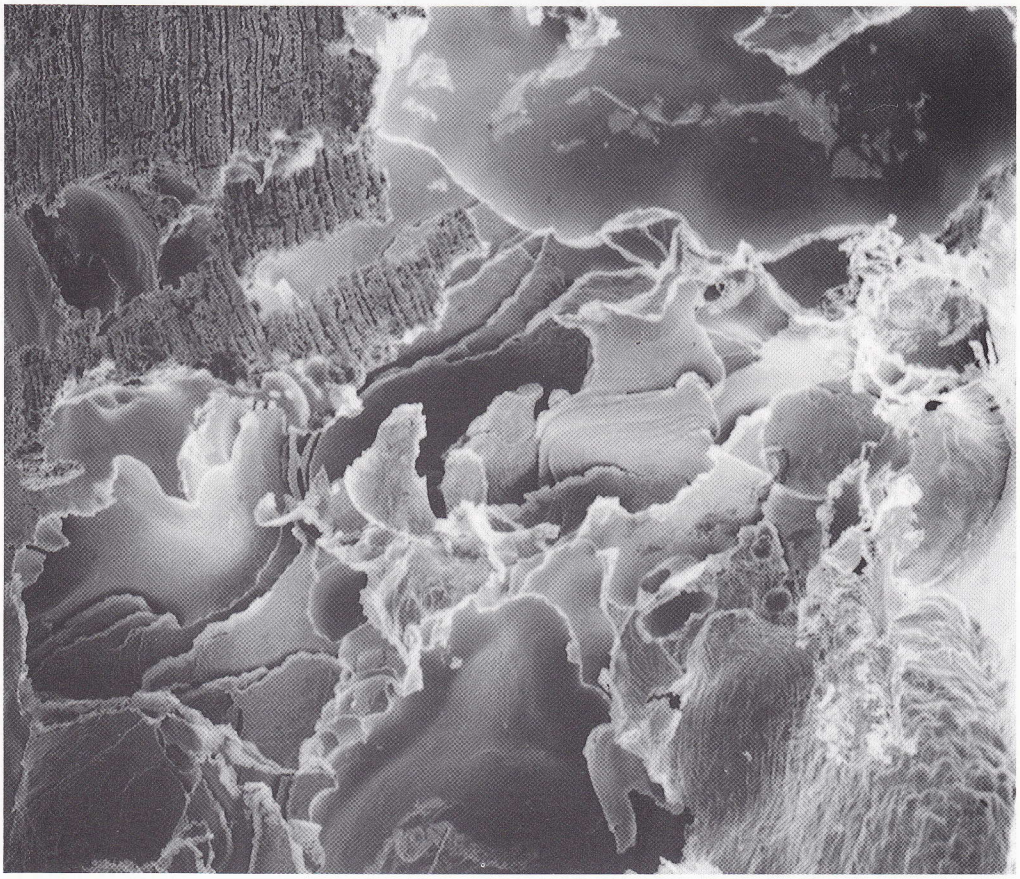

Fig. 4

Fig. 5a

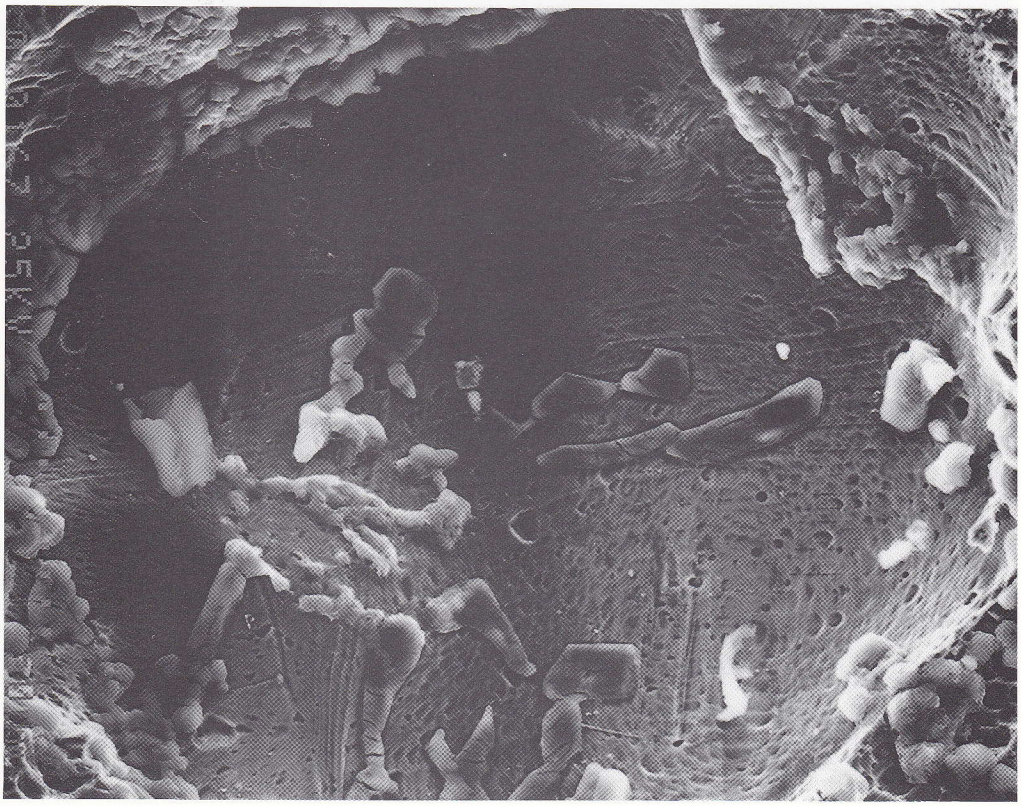

Fig. 5b

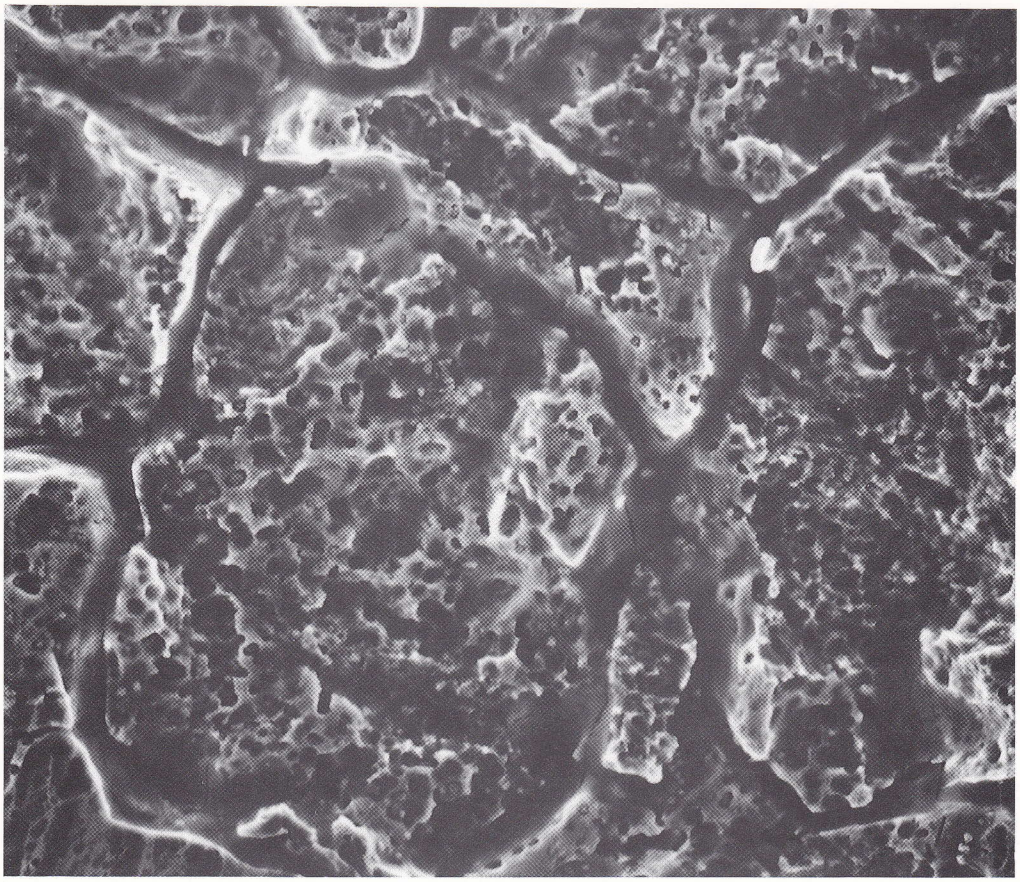

Fig. 6

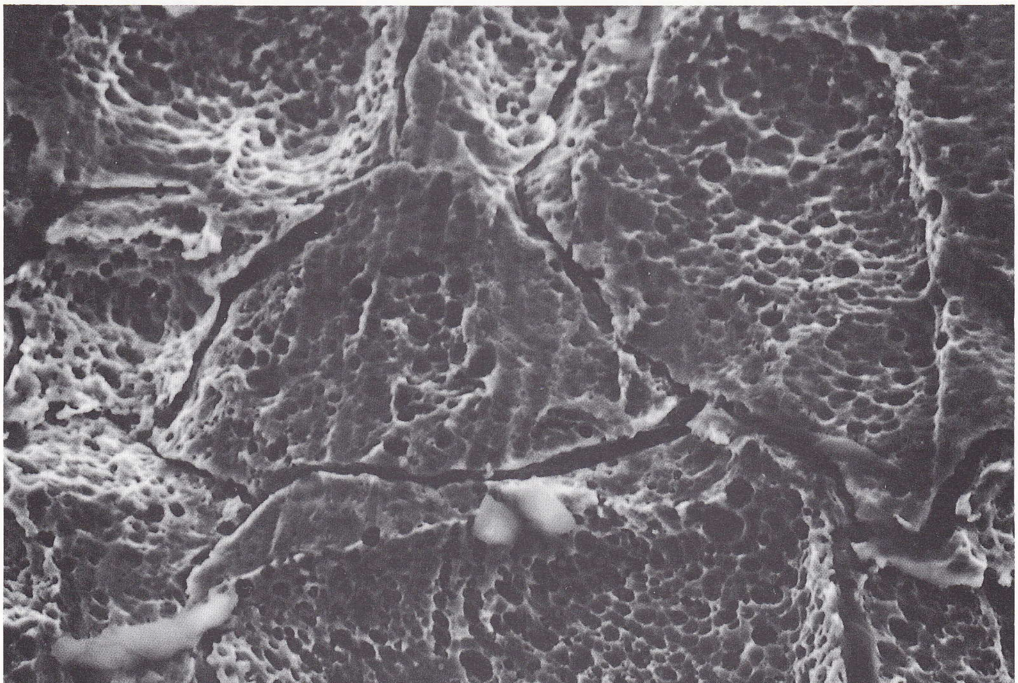

Fig. 7